2.6 FAIR WEATHER CLIMATOLOGY REVEALED BY THE CCNY LIDAR

Stanley David Gedzelman*, Kwan-yin Kong, Fred Moshary, Heather Yael Glickman, Barry Gross, and Leona Charles
NOAA Crest Center, City College of New York, New York, NY 10031

1. INTRODUCTION

Remote sensing of the atmosphere by instruments including **LIDAR** (**LI**ght **D**etection **A**nd **R**anging) has greatly improved weather forecast accuracy and our ability to assess human impact on the environment. Important uses of lidar in the atmosphere have been to detect gases, (e. g., H_2O) and aerosol and cloud particles, as in cirrus (Wang and Sassen, 2002).

Lidar is a valuable tool for weather analysis, when used with standard meteorological measurements, as well as by radar and satellite imagery. For example, lidar enables continuous, precision monitoring of Atmospheric Boundary Layer (ABL) structure (Menut, et. al., 1999).

The City College (CCNY) vertically pointing Lidar was installed in June 2004 in the aftermath of the 9/11 tragedy to monitor the atmospheric environment over New York City. It operates at three wavelengths (355, 532, and 1064 nm), providing 1-minute soundings from 500 m to 15 km with vertical resolution, 10 m. Images display the logarithm of Range Corrected Power (RCP) of the lidar signal after Rayleigh scattering of the molecular atmosphere has been subtracted. Raman Lidar capability was added in Oct 2006 but is not included in this analysis.

In the course of analyzing lidar profiles to detect and track aerosol layers aloft, a variety of local and mesoscale cloud and weather features such the Atmospheric Boundary Layer (ABL), frontal passages, sea breezes and high clouds were identified and analyzed (Gedzelman, et. al. 2006). Here, we present a fair weather lidar climatology and focus on 2 cases that illustrate the meteorological content of the lidar profiles.

2. LIDAR CLIMATOLOGY

The CCNY Lidar climatology is based on vertical time section images for 187 days (as of 16 Oct 2006). Each day began with skies not under a low or mid level overcast. Largely as a result of this sampling criterion, few mid-level clouds were detected. Most low clouds were cumulus or stratocumulus while most high clouds were cirrus.

The ABL is the most prominent and common feature of the lidar profiles. In most cases it is marked by an abrupt reduction in RCP. Lidar based ABL heights (Fig. 1) closely agree with heights based on soundings obtained from the ARL/NOAA HYSPLIT model. A distinct annual cycle of ABL heights is present, with higher mean values from about Julian days 80 to 240 (spring and summer) and lower values in fall and winter, when solar heating is weaker.

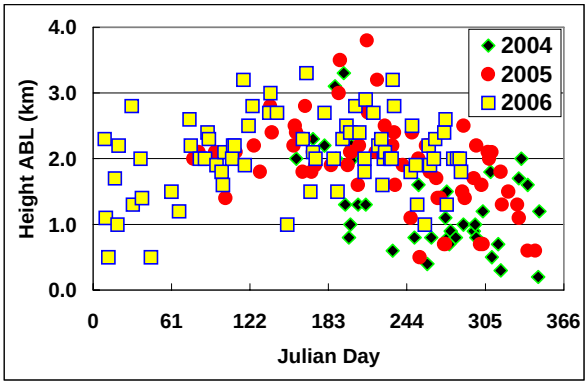

Fig. 1. Maximum ABL heights for each CCNY Lidar time section.

On a typical sunny day, the ABL gradually evolves from a thin layer with an indefinite top in the morning to a thick layer with a distinct. The ABL is often capped by scattered cumulus by mid afternoon. On about 10 spring and summer days each year, ABL thickness increased rapidly, indicating passage of a sea breeze front. On many of these days the front was marked by an EW line of cumulus over Long Island.

Distinct, elevated aerosol layers above the ABL were present in 82% of the profiles in 2005 and 2006 (image quality in 2004 was not fine enough to detect layers with small opacity). Waves with typical periods of 10 min and double amplitudes up to about 300 m were present on 72% of the elevated aerosol layers and were also

❖ *Corresponding Author Address:* Stanley David Gedzelman, Department of Earth and Atmospheric Sciences, City College of New York, New York, New York, 10031 Email: sgedzelman@ccny.cuny.edu

seen in aerosol layers within or at the top the ABL. Aerosol layers with the highest RCP tended to 1: contain the most prominent waves and, 2: derive from major events such as forest fires in Alaska (21 July 2004), Canada (07 July 2006 – see Fig. 2; Hoff, et. al., 2007) and dust storms in the Gobi Desert (10 May 2005, 19 Apr 2006). For the last date, Charles, et. al. (2007) documented that PM 10 aerosol number density at ground level in NYC spiked more than 100% shortly after elevated aerosol layers descended into the ABL. PM 10 is a typical size for desert dust (Prospero, et. al, 2001). About 20 other cases of elevated aerosol layers that entered the ABL over NYC were recorded in 2005 and 2006 and await analysis.

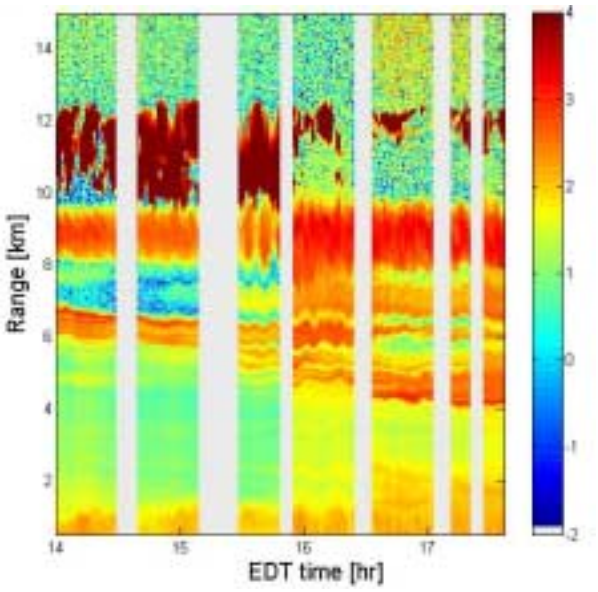

Fig. 2. CCNY Lidar time section, 07 July 2006 of log of range corrected power (colors). Dark red region from 10-12 km is cirrus. Orange-red veneers from 4 – 9.5 km are aerosol layers from Canadian fires. Waves on the aerosol layers had the largest amplitude of all profiles. Note also thickening of the ABL as yellow veneers sink into it at 1630 EDT.

3. CASE STUDIES

Case studies are presented here to illustrate the meteorological content implicit in the lidar profiles. Clouds appear opaque at all 3 wavelengths. By contrast, most aerosol layers are almost invisible at 355 nm. The identification as a cloud or an aerosol layer is then checked by using HYSPLIT soundings and the cloud form is verified using MODIS images. Back trajectories are used to determine regions of origin of clouds or aerosol layers. In cases where knowledge of fine scale structure is needed, as when short-period waves or sea breeze fronts occur, the WRF model is run with resolution of 2 km.

Case 1: Sea Breeze Front of 13 June 2006

From 1800 to 1900 UTC on 13 June 2006, ABL thickness increased from about 1 to 2.2 km (Fig. 3) as a sea breeze front passed over CCNY. A line of cumulus formed where surface winds converged at the leading edge of the front (Fig. 4).

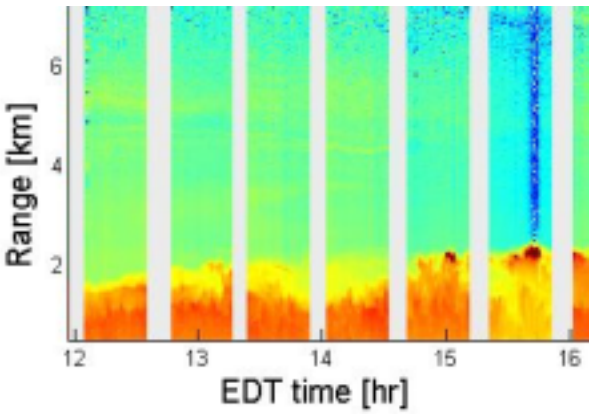

Fig. 3. Lidar profile, 13 June 2006 up to 4 km from 1400 to 1630 EDT showing increase of ABL thickness (orange or red) at time of sea breeze passage. Dark pixels indicate cumulus bases.

Fig. 4 MODIS AQUA image, 1740 UTC on 13 June 2006 showing cumulus cloud line at sea breeze front on Long Island.

These features were simulated by a WRF model run for 24 hours beginning 0000 UTC, 13 June 2006. The vertical cross section (not shown) indicated that as the sea breeze front formed and moved inland, the ABL rose everywhere about 0.5 km and an E-W line of cumulus (gray) formed

over western Long Island at the convergence line at the leading edge of the maritime air (Fig 5). The gradual rise of the ABL on both sides of the sea breeze front suggests that in this case the front did not advance in the manner of a hydraulic jump.

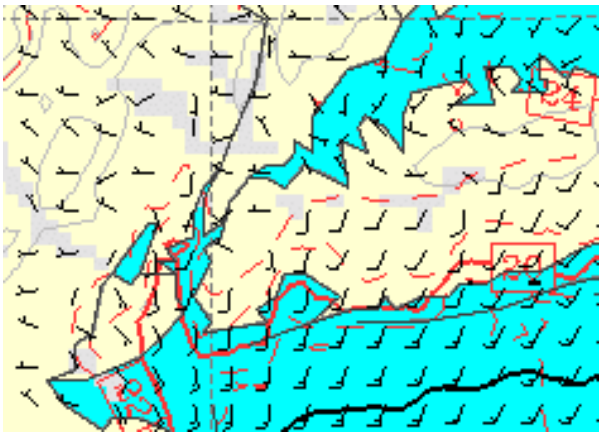

Fig. 5. WRF generated surface map at 2200 UTC on 13 June 2006 showing wind (barbs), clouds (gray shading), T (ºC - red lines) and heights (gray lines).

Case 2: Wavy Gobi Dust Layers 19 April 2006

The CCNY Lidar profile for 19 April 2006 revealed heavy aerosol loading up to about 6km Fig. 6). Charles, et. al. (2007) showed that the aerosols derived from a Gobi Desert dust storm and that some entered the ABL over NYC.

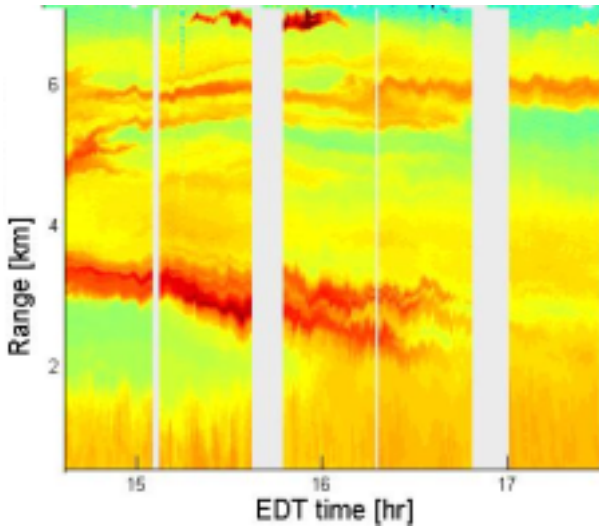

Fig. 6 CCNY Lidar Profile, 19 April 2006 with wavy lamina from Gobi Desert Dust Storm.

The layer contained distinct lamina with waves of periods 5 to 10 min and double amplitudes up to 300 m. Skies were clear over NYC but standing wave clouds were observed to the NE over southern New England (Fig. 7).

Fig. 7. MODIS AQUA image, 1740 UTC 19 Apr 2006 showing standing wave clouds to the NE of NYC over Connecticut.

The WRF model for this case generated a series of standing mountain waves shown in the cross section of Fig 8. The simulated 850 hPa chart (Fig. 9) contained roughs and crests properly oriented from WNW to ESE but largest amplitudes over and downwind from the Catskill Mountains instead of in Southern New England.

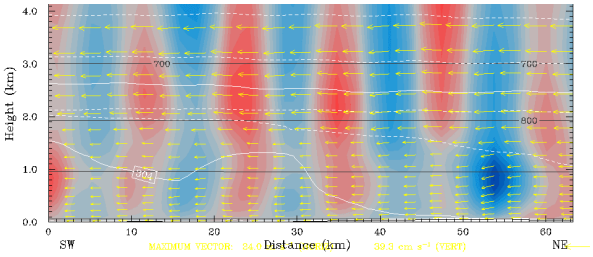

Fig. 8. WRF generated cross section, 1800 UTC 19 April 2006 extending from SSW to NNE with CCNY at the center. Colors indicate vertical velocity (red = rising, blue = sinking). Maximum values ≈ 0.75 m

Because a vertically pointing time section can only show travelling waves, waves on the aerosol lamina had to have formed upwind, for example, over mountains or at the source. The wavy lamina were then advected with the wind. Given the prevalence of similar travelling waves on aerosol layers in the CCNY Lidar profiles, often during times when standing mountain waves are

observed upwind, the origin and nature of the waves on the lamina is a matter of interest.

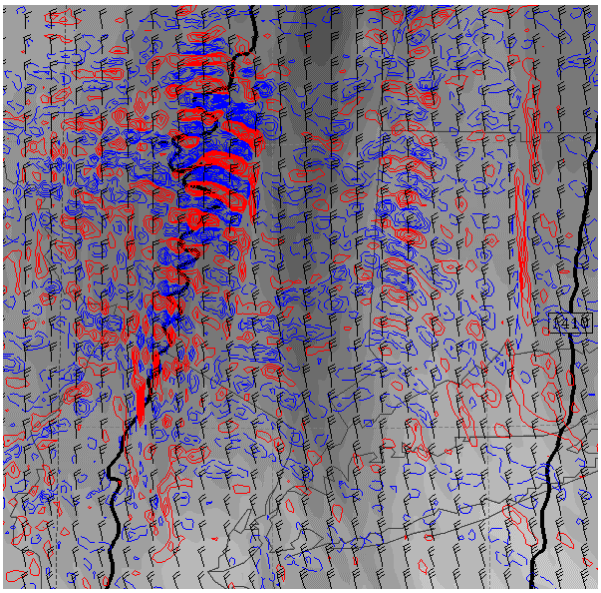

Fig. 9. WRF generated 850 hPa chart, 1800 UTC 13 June 2006 showing vertical velocity (red = rising, blue = sinking) and relative humidity (dark = low, light = high).

Acknowledgments. The authors thank the CCNY staff and students who vigilantly maintain the CCNY Lidar. The first author benefited from discussions on desert dust with Dr. Joe Prospero, U, Miami. This research is sponsored by a NOAA CREST grant.

REFERENCES

Charles, L., S. et. al., 2007: Application of CCNY Lidar and ceilometers to the study of Aerosol Transport and PM2.5 monitoring. *Amer. Meteor. Soc*., *3rd Symposium on Lidar Atmospheric Applications*.

Hoff, R., M, et. al., 2007: Lidar validation of CALIPSO and OMI using ground-based sensors from REALM. *Amer. Meteor. Soc*., *3rd Symposium on Lidar Atmospheric Applications*.

Gedzelman, S. D., et. al., 2006: Mesoscale weather features in NYC revealed by CCNY Lidar. *Amer. Meteor. Soc*., *6th Symposium on the Urban Environment*.

Menut, L., C., et. al., 1999: Urban boundary layer height determination from lidar measurements over the Paris area. *Appl. Opt*., **38**, 945-954.

Prospero, J. M., et. al., 2001: Al and Fe in PM 2.5 and PM 10 suspended particles in south-central Florida: The transport of African mineral dust. *Water, Air, Soil Poll.,* **125:** 291–317, 2001.

Wang, Z., and K. Sassen, 2002: Cirrus cloud microphysical property retrieval using lidar and radar measurements: I. Algorithm description and comparison with in situ data. *J. Appl. Meteor*., 41, 218-229.